ISSN 1063-7842, Technical Physics, 2018, Vol. 63, No. 9, pp. 1270–1276. © Pleiades Publishing, Ltd., 2018.
Original Russian Text © A.N. Korshunova, V.D. Lakhno, 2018, published in Zhurnal Tekhnicheskoi Fiziki, 2018, Vol. 88, No. 9, pp. 1312–1319.

PHYSICAL APPROACHES AND PROBLEMS OF DATA INTERPRETATION IN THE LIFE SCIENCES

Simulation of the Stationary and Nonstationary Charge Transfer Conditions in a Uniform Holstein Chain Placed in Constant Electric Field

A. N. Korshunova[a,*] and V. D. Lakhno[a]

[a] *Institute of Mathematical Problems in Biology, Federal Research Center Keldysh Institute of Applied Mathematics, Russian Academy of Sciences, Pushchino, Moscow oblast, 142290 Russia*

**e-mail: alya@impb.ru*

Received January 13, 2018

Abstract—The charge transfer in a Holstein molecular chain placed in a uniform electric field has been numerically simulated. It has been shown that for given parameters of the chain, a charge placed in a constant electric field may uniformly travel very large distances (several hundred thousand sites). The charge may move with a constant velocity if the field strength is low. With an increase in the field strength, the charge starts oscillating (Bloch oscillations). Good agreement has been shown between the theoretical and numerical field dependences of the charge constant velocity.

DOI: 10.1134/S1063784218090086

INTRODUCTION

Interest in charge transfer in 1D molecular chains is associated with the possible use of these chains as wires in nanoelectronic devices. In 1D chains, self-trapped electron states (appearing as polarons) serve as charge carriers. The question of whether localized excitations, solitons, and polarons, can transfer energy and charge in biological molecules, such as proteins, was discussed by Davydov [1–4]. In view of advances in molecular nanobioelectronics, the main purpose of which is designing electron devices based on biomolecules [5, 6], researchers concentrate on the problem of charge transfer in extended molecules such as a DNA molecule [7–15].

In this work, we report numerical simulation data for charge transfer in a polynucleotide Holstein molecular chain placed in a constant electric field. Earlier [16], one of the authors considered this issue for a continuous chain. Clearly, data obtained in [16] may be inapplicable to a discrete chain. Moreover, motions that arise in the discrete case may be absent entirely in the continuous case.

DYNAMIC MODEL OF A DISCRETE HOLSTEIN CHAIN

In the model of a polynucleotide Holstein molecular chain that follows, the chain is assumed to consist of N sites. Each site is a nucleotide pair that is considered as a harmonic oscillator [17]. To simulate the quantum dynamics of a particle in a chain of N nucleotide pairs, we will use the Holstein Hamiltonian. Holstein was the first to consider a chain each site of which represents a diatomic molecule [17, 18]:

$$\hat{H} = -\sum_{n}^{N} \nu(|n\rangle\langle n-1| + |n\rangle\langle n+1|) + \sum_{n}^{N} \alpha q_n |n\rangle\langle n| + \sum_{n}^{N} M\dot{q}_n^2/2 + \sum_{n}^{N} kq_n^2/2 + \sum_{n}^{N} e\mathscr{E}n|n\rangle\langle n|. \quad (1)$$

Here, ν is the matrix element of charge transfer between neighboring sites (nucleotide pairs), α is the constant of interaction between the charge and displacements q_n, M is the effective mass of the site, and k is the elastic constant.

Equations of motion for Hamiltonian $\hat{H}$ lead us to the set of differential equations

$$i\hbar\dot{b}_n = -\nu(b_{n-1} + b_{n+1}) + \alpha q_n b_n + \varepsilon\mathscr{E}anb_n, \quad (2)$$

$$M\ddot{q}_n = -\gamma\dot{q}_n - kq_n - \alpha|b_n|^2, \quad (3)$$

where b_n is the amplitude of the probability that the charge is in the nth site, $\sum_n |b_n|^2 = 1$. Classical equation of motion (3) contains friction coefficient γ, which stands for dissipation.

Equations (2) (where $\hbar = h/2\pi$ and h is the Planck constant)) are Schrödinger equations for probability amplitudes b_n, which describe the evolution of the particle in the deformed chain, and Eq. (3) is a classical equation of motion that describes the dynamics of polynucleotide pairs with regard to dissipation.

In Eqs. (2) and (3) we now pass to dimensionless variables using the relationships

$$\eta = \tau\nu/\hbar, \quad \omega^2 = \tau^2 K/M,$$
$$\omega' = \tau\gamma/M, \quad q_n = \beta u_n, \quad E = \mathscr{E} ea\tau/\hbar, \qquad (4)$$
$$\kappa\omega^2 = \tau^3(\alpha)^2/M\hbar, \quad \beta = \tau^2\alpha/M, \quad t = \tau\tilde{t},$$

where τ is the reduced scale of time that relates time t and dimensionless variable $\tilde{t}$.

In dimensionless variables (4), Eqs. (2) and (3) take the form

$$i\frac{db_n}{d\tilde{t}} = -\eta(b_{n+1} + b_{n-1}) + \kappa\omega^2 u_n b_n + Enb_n,$$
$$\frac{d^2u_n}{d\tilde{t}^2} = -\omega_n' \frac{du_n}{d\tilde{t}} - \omega_n^2 u_n - |b_n|^2. \qquad (5)$$

The model thus introduced is the simplest model describing the dynamics of a charged particle in a polynucleotide chain and taking into account dissipation in the system in explicit form.

SIMULATION OF THE UNIFORM CHARGE MOTION IN A CONSTANT ELECTRIC FIELD

Obviously, simulation of the particle dynamics even in a uniform $(G)_n$ chain is a multiparametric problem, which necessitates a large amount of computation for different values of the chain parameters. The selection of the system's parameters to simulate specific behavior of the charge in an electric field is accomplished both according to the results of system analysis in continuum limit [19] and based on numerical simulation data. Having selected model parameters of the chains, we can study the charge transfer and charge distribution with a computation speed much higher than in the case of real DNA chains.

The charge transfer in an electric field was simulated with the following dimensionless parameters: $\kappa = 1$, $\eta = 1.276$, and $\omega = 1$. With these values fixed, we vary friction coefficient ω' in the chain and electric field strength E. Computation was carried by the standard Runge–Kutta fourth-order method. To simulate the uniform motion of charge in an electric field, its value was initially (at zero time) set equal to the value that follows from a stationary solution to Eqs. (2) and (3) in the absence of the electric field; that is, the initial values of $|b_n(0)|$ were taken in the form of the inverse hyperbolic cosine:

$$|b_n(0)| = \frac{\sqrt{2}}{4}\sqrt{\frac{\kappa}{|\eta|}}\cosh^{-1}\left(\frac{\kappa(n-n_0)}{4|\eta|}\right), \qquad (6)$$
$$u_n^0 = |b_n(0)|^2/\omega_n^2,\ du_n^0/d\tilde{t} = 0.$$

Let us now assume that the characteristic size of the charge distribution is given by

$$d(\tilde{t}) = \sum|b_n(\tilde{t})|^2 / \sum|b_n(\tilde{t})|^4 = 1/\sum|b_n(\tilde{t})|^4. \qquad (7)$$

For the given values of the chain parameters, the characteristic size of the polaron in the chain is determined as $\lim_{\tilde{t}\to\infty} d(\tilde{t}) \approx 15$. That is, for these parameters of the chain, the polaron is wide and covers a large number of sites. The value of n_0 (the center of the charge initial distribution) in (6) was taken so that the polaron was far from the end of the chain at the beginning of computation. Similarly, the length of the chain was selected so that the polaron remained sufficiently far from the chain by the end of computation. The field was assumed to be switched on instantly at the initial instant of time.

The reasonable question arises as to at which field strengths E the charge motion in the chain becomes uniform for the given values of the parameters. A relationship between the uniform velocity of a polaron, $V = va/\tau$, and the electric field strength in the continuum limit was considered elsewhere [19]. For the undamped motion of nucleotide pairs, when the friction coefficient is low, $\omega > \omega'/2$, the following relationship between polaron equilibrium velocity V and electric field strength E [19]:

$$E = \kappa\omega^2\omega' VI, \quad E = \mathscr{E}\frac{ea\tau}{\hbar},$$
$$I = \frac{2\eta}{\kappa V^4}\int_0^\infty \frac{x^4/\sinh^2 x}{(x^2 + c_1) + c_2^2}dx,$$
$$c_1 = \left(\frac{2\pi\eta}{\kappa V}\right)^2\left(\frac{\omega'^2}{2} - \omega^2\right), \qquad (8)$$
$$c_2^2 = \left(\frac{2\pi\eta}{\kappa V}\right)^4\omega'^2\left(\omega^2 - \left(\frac{\omega'}{2}\right)^2\right).$$

In the case of the damped motion of nucleotide pairs ($\omega'/2 > \omega$), quantity I is given by [19]

$$I = \frac{2\eta}{\kappa V^4}\int_0^\infty \frac{x^4/\sinh^2 x}{(x^2 + c_1^2)(x^2 + c_2^2)}dx,$$
$$c_1 = \frac{2\pi\eta}{\kappa V}\left(\frac{\omega'}{2} - \sqrt{\left(\frac{\omega'}{2}\right)^2 - \omega^2}\right), \qquad (9)$$
$$c_2 = \frac{2\pi\eta}{\kappa V}\left(\frac{\omega'^2}{2} + \sqrt{\left(\frac{\omega'}{2}\right)^2 - \omega^2}\right).$$

The limiting case when friction is absent was touched upon in [20]. In this work, we consider the polaron velocity V versus field strength E dependence at different friction coefficients ω'.

Figure 1 plots the polaron velocity versus the field strength dependences (see (8), (9)) for different values of parameter ω' and $\kappa = 1$.

The first four curves on the left of Fig. 1 correspond to the damped motion of nucleotide pairs given by (9) for $\omega'/2 > \omega$, namely, for $\omega' = 6$, 4, 3, and 2. The next five curves describe the undamped motion of the pairs

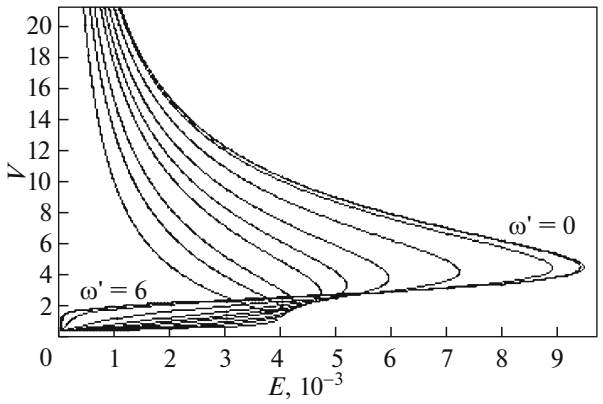

Fig. 1. Polaron velocity V vs. electric field strength E for $\kappa = 1$; $\eta = 1.276$; $\omega = 1$; and $\omega' = 6, 4, 3, 2, 1.5, 1, 0.5, 0.1, 0.01, 0$.

given by (8): $\omega'/2 < \omega$, $\omega' = 1.5, 1.0, 0.5, 0.1$, and 0.01. The limiting case $\omega' = 0$ considered in [20] is represented by the rightmost curve, whereas the limiting case $\omega' = \infty$ is represented by the vertical axis. It follows from Fig. 1 that the soliton may move uniformly only if $0 < E < E_{max}(\omega')$. In each curve, the branch for which the inequality $dV/dE = V'_E > 0$ is valid corresponds to the stable motion of the soliton, whereas the branch for which $V'_E < 0$ describes the unstable motion. From (8) and (9) it is seen that friction gives rise to an ohmic portion, i.e., to a linear portion in the stable branches of the $V(E)$ curves at low E.

Figure 2 plots function

$$X(\tilde{t}) = \sum_n |b_n(\tilde{t})|^2 n, \qquad (10)$$

which describes the motion of the center of mass of the particle. These plots demonstrate that the $\tilde{t}$ dependence is linear for almost all values of the electric field strength E (Fig. 2). It is distinctly seen that the leftmost plot $X(\tilde{t})$ for $E = 0.0012$ ($\mathscr{E} = 2.256 \times 10^3$ V/cm) deviates significantly from a straight line. This means that the charge executes oscillatory motion. Thus, it was found that for fields $E > 0.0011$ and the selected values of the chain parameters, the charge cannot move uniformly.

Figure 3 plots functions $|b_n(\tilde{t})|$ and $X(\tilde{t})$ for electric field strength $E = 0.001$. At the initial instant of time, the polaron is in site $n_0 = 601$. This is an example of the uniform motion of the charge along the chain. In addition, the example shown in Fig. 3 correlates with the third plot on the left of Fig. 2, which also corresponds to $E = 0.001$.

Fragments of the polaron velocity V versus external field E dependence are shown in Figs. 4 and 5. They provide a deeper insight into the stable motion of the soliton ($dV/dE = V'_E > 0$). Figure 5 represents the real part of Fig. 4. It follows from the plots that the linear

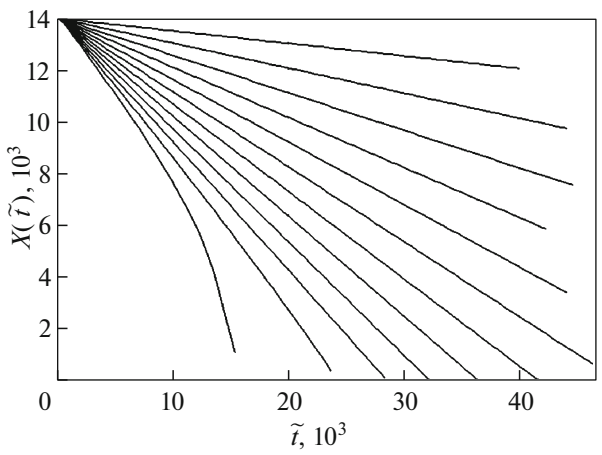

Fig. 2. Plots of function $X(\tilde{t})$ for $\kappa = 1$; $\eta = 1.276$; $\omega = 1$; $\omega' = 1$; dimensionless time $\tilde{t} = 47000$; and $E = 0.0001$, 0.0002, 0.0003, ..., 0.0012. The chain length equals 15 001 site. The uppermost curve is plotted for $E = 0.0001$.

portion extends with ω'. At $\omega' \gtrsim 1$ (for $\kappa = 1$), the linear portion of the field dependence of the soliton velocity extends up to the critical value of the electric field, at which the uniform motion of the soliton becomes impossible. In this case, the Ohm law is fulfilled with a high accuracy up to very high electric fields.

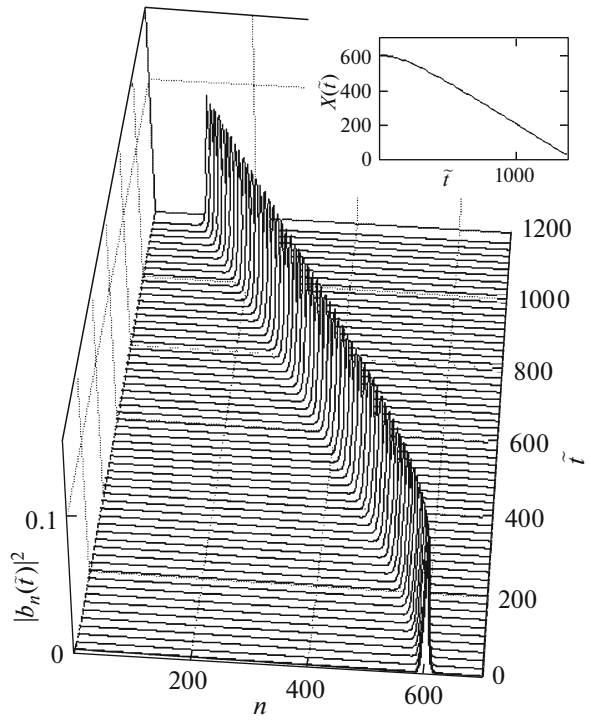

Fig. 3. Plots of functions $|b_n(\tilde{t})|$ and $X(\tilde{t})$ for $\kappa = 1$; $\eta = 1.276$; $\omega = 1$; $\omega' = 1$; dimensionless time $\tilde{t} = 1200$; and $E = 0.001$. The chin length equals 701 site.

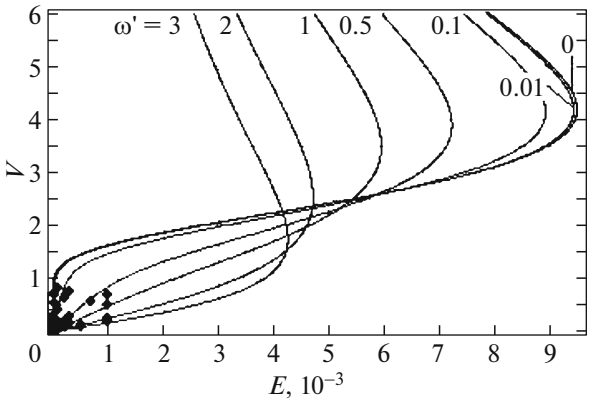

Fig. 4. Soliton velocity V vs. electric field strength E for $\kappa = 1$; $\eta = 1.276$; $\omega = 1$; and $\omega' = 3, 2, 1, 0.5, 0.1, 0.01, 0$. The plots correspond to the stable motion of the soliton ($dV/dE = V'_E > 0$).

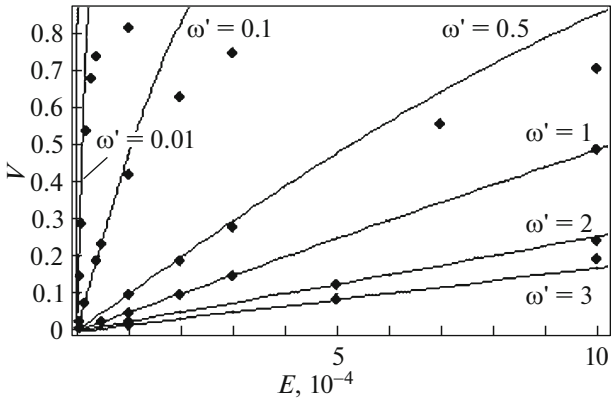

Fig. 5. (—) Theoretical (expressions (8), (9)) vs. (●) numerically simulated field dependence of soliton velocity V for $\kappa = 1$; $\eta = 1.276$; $\omega = 1$; and $\omega' = 3, 2, 1, 0.5, 0.1, 0.01, 0$. The linear portions of the $V(E)$ curves are shown.

Figure 4 compares the numerical (●) and "theoretical" dependences of soliton velocity V on electric field E. It should be noted that here the limiting case $\omega' = 0$ is described by the leftmost curve. From Figs. 1 and 4 it follows theoretically that the charge can move uniformly if E is within the interval $0-E_{max}(\omega')$, It is seen in the plots that point $E_{max}(\omega')$ correlates with the inflection point in the $V(E)$ curve. However, numerical experiment data show that the charge motion can be uniform in the interval $0 < E < E_{max\text{-}numerical}(\omega')$, which is much shorter than $0 < E < E_{max}(\omega')$. In the interval $E > E_{max\text{-}numerical}(\omega')$, the uniform motion of the charge is not observed (Fig. 2).

SIMULATION OF THE NONUNIFORM CHARGE TRANSFER IN A CONSTANT ELECTRIC FIELD

Calculations show that for $E > E_{max\text{-}numerical}(\omega')$, as well as for $E > E_{max}(\omega')$, the charge as a whole executes Bloch oscillations at the beginning of motion and then loses its initial shape. The higher E and the greater the difference between E and $E_{max\text{-}numerical}(\omega')$, the quicker the charge initial distribution deviates from its initial form (inverse hyperbolic cosine, see (6)). Then, the charge moves in the direction of the field, continuing to oscillate with a period close to the period of Bloch oscillations: $T_{BL} = 2\pi/E$. No singularities in the motion of the particle in the field when E becomes greater than $E_{max}(\omega')$ were observed.

When simulating the nonuniform charge motion (as in the above case of its uniform motion), we placed a charge corresponding to a stationary solution to Eqs. (2) and (3) in a chain at zero time, assuming that the field is absent. The initial values of $|b_n(0)|$ were also taken in the form of the inverse hyperbolic cosine (see (6)). However, the values of the field strength E were taken large.

Figure 6 plots function $X(\tilde{t})$ for different values of field strength E starting from $E = 0.001$. In Fig. 6 this value of E corresponds to a straight line, which means that the motion of the charge in the chain is uniform. The rest of the plots correspond to oscillatory regimes of the charge transfer. The period of Bloch oscillations for $E = 0.001$ is equal to $T_{BL} = 2\pi/E \approx 6283$. It then follows that the plot for $E = 0.001$ covers 3.6 of Bloch periods. That is, this plot does indicate that the motion of the charge is uniform, rather than being part of the oscillatory motion of the polaron. It should be noted that Fig. 2 also contains a plot constructed for $E = 0.001$ (the third curve from the left). It covers time span $\tilde{t} \approx 28000$, which is roughly equal to 4.5 Bloch periods.

The plots describing the oscillatory motions in Fig. 6 clearly demonstrate that the oscillation period decreases with increasing field strength and is always roughly equal to $T_{BL} = 2\pi/E$. Of interest is the curve $X(\tilde{t})$ constructed for $E = 0.002$ in Fig. 6. This is the lowest curve, exclusive of the curve for $E = 0.001$. Its shape for $\tilde{t} > 10000$ is incorrect in the sense that the charge has already begun to reflect from the left end of the chain, as is distinctly seen in Fig. 6. Moreover, if the charge as a whole is involved in oscillatory motion at the initial instant of time (as in the given case), its center of mass shifts by the maximal Bloch amplitude: $A_{BL} = 4\eta/E$. For $E = 0.002$, the maximal Bloch amplitude is $A_{BL} = 4\eta/E \approx 2500$. However, from Fig. 6 it follows that the center of mass of the polaron shifted by 4000 sites at once. Actually, at $E = 0.002$, the polaron moves uniformly almost at once at instant field switching, slightly declining, and, having passed about 1500, becomes completely involved in Bloch oscillations. It departs by maximal Bloch amplitude $A_{BL} = 4\eta/E$ after the beginning of motion only starting from $E = 0.005$.

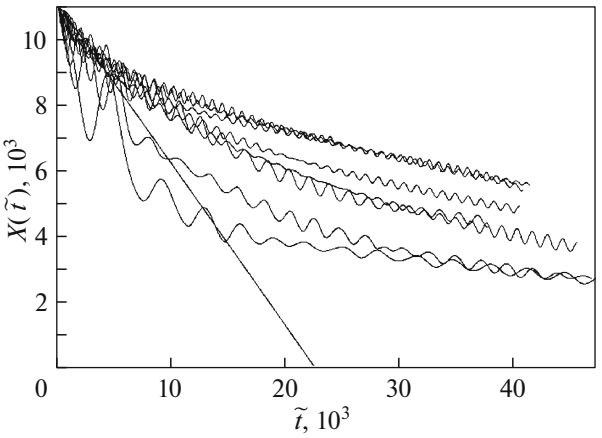

Fig. 6. Plots of function $X(\tilde{t})$ for $\kappa = 1$; $\eta = 1.276$; $\omega = 1$; $\omega' = 1$; and $E = 0.001$, 0.002, 0.003, ..., 0.008; and a dimensionless time of 47 000. The chain length is $N = 12001$ site.

Figure 7 exemplifies the motion of the polaron in a chain $N = 701$ long for a high electric field strength, $E = 0.03$. For $E = 0.03$, the period of Bloch oscillations $T_{BL} = 2\pi/E \approx 209$. An initial polaron given by (6) is typically 15 long and about 0.1 high. In the absence of the field, such an initial polaron state remains virtually unchanged and the polaron does not change its initial position infinitely long, since friction in the given chain is high. It should be noted that if friction in the chain is absent or very low, the polaron retains its initial position only when it is at the center of the chain [21, 22]. Since friction in the given chain is high and the polaron does not change its initial position in the absence of the field, the charge localizes within one maximal Bloch amplitude in the direction of the field at instantaneous field switching during the first oscillation.

The plots of function $|b_n(\tilde{t})|^2$ clearly demonstrate how the initial polaron given by (6) quickly decays, moving along the field in the chain and executing Bloch oscillations. Also, it is distinctly seen in Fig. 7 that the charge during the last (fifth) oscillation reflects from the end of the chain, rather than from its boundary, as in the previous oscillations.

The charge transfer in the electric field strongly depends on the charge initial distribution in the chain. The motion of the charge that is initially in the polaron state (see (6)) is exemplified in Fig. 7. Let us see how the charge occupying one site behaves in the field. We place the charge in one site at the center of the chain. The distribution of this charge over the chain without the field is shown in Fig. 8. A straight line passing through the center of Fig. 8 shows the unit charge at the center of the chain for a left scale of 0.12. It is well seen that the charge quickly spreads in the chain, reflecting from the ends of the chain, and finally becomes uniformly distributed over the chain.

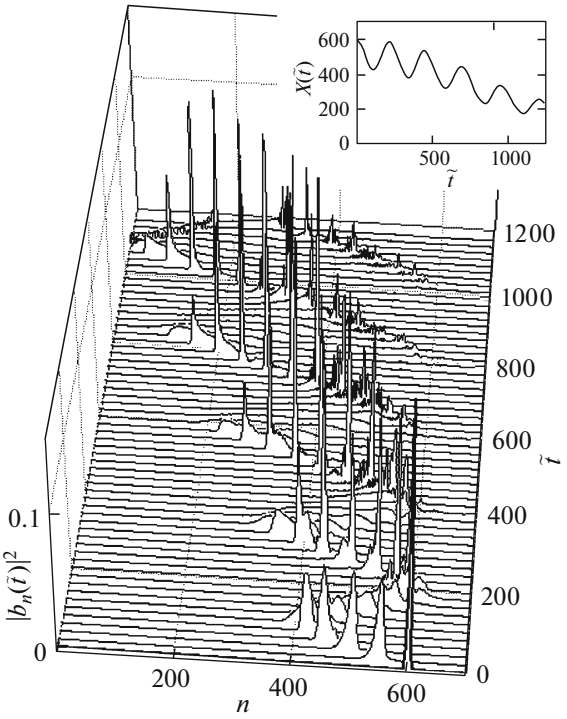

Fig. 7. Plots of functions $|b_n(\tilde{t})|^2$ and $X(\tilde{t})$ for $\kappa = 1$, $\eta = 1.276$, $\omega = 1$, $\omega' = 1$, $E = 0.03$, and a dimensionless time of 1200. The chain length is $N = 701$ site.

In the presence of the field, the distribution of the unit charge is quite different. In Fig. 9, at the initial instant of time, the charge occupies one site at the center of the chain, the field is switched instantly at the initial instant of time, and the field strength is the same as in Fig. 7 ($E = 0.03$). The plots of function $|b_n(\tilde{t})|^2$ demonstrate that the charge does not spread over the chain in the presence of the field.

The initial unit charge first spreads on either side of the center but soon localizes within one maximal Bloch amplitude under the action of the electric field. Then, the charge moves along the chain, executing Bloch oscillations with a period close to the Bloch period for the given electric field strength ($E = 0.03$). Here, the type and velocity of motion much differ from those in Fig. 7.

Numerical simulation data indicate that for the given parameters, the type and velocity of charge transfer in the field strongly depend on the characteristic size both of the charge initial distribution and of the stationary polaron in the chain. The examples given in Figs. 7 and 9 show how different initial distributions of the charge influence the subsequent charge distributions over the chain in the case of oscillatory motion.

For $\kappa > 1$ ($\eta = 1.276$), the charge motion may be both uniform and oscillatory depending on charge initial distribution (6) with the chain parameters and

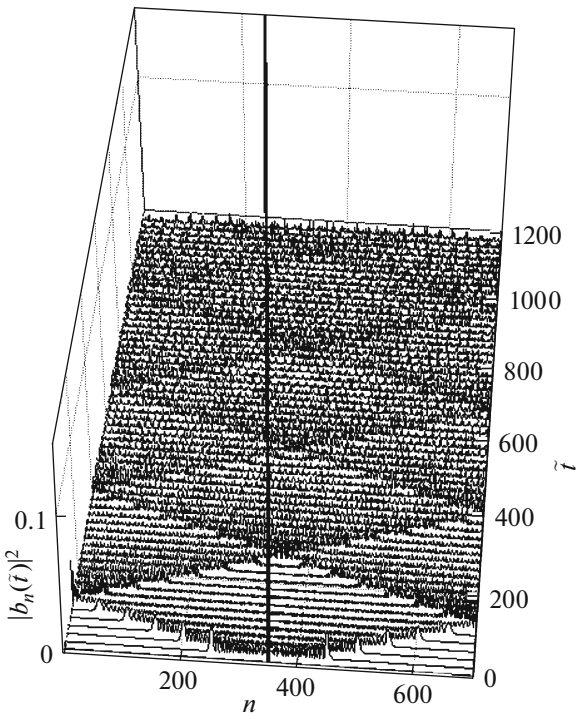

Fig. 8. Plots of functions $|b_n(\tilde{t})|^2$ and $X(\tilde{t})$ for $\kappa = 1$, $\eta = 1.276$, $\omega = 1$, $\omega' = 1$, and a dimensionless time of 1200 in the absence of the electric field. The chain length is $N = 701$ site. Initially, the charge is within one site at the center of the chain. $u_n^0 = 0$ for all n.

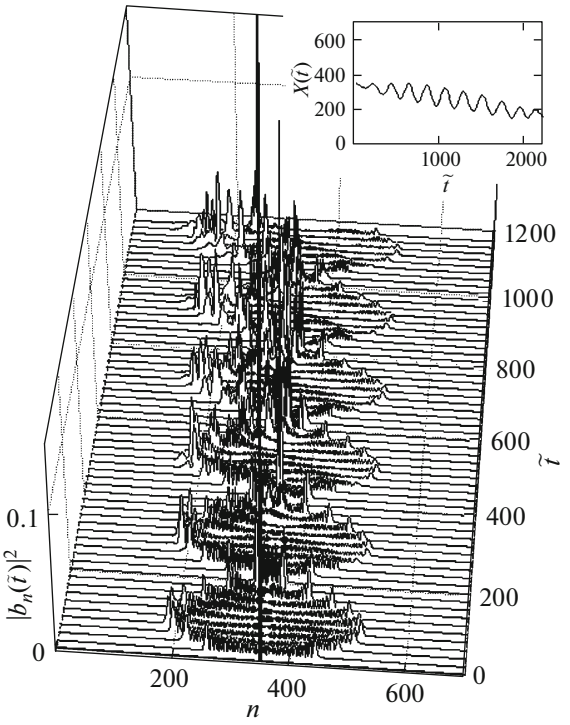

Fig. 9. Plots of functions $|b_n(\tilde{t})|^2$ and $X(\tilde{t})$ for $\kappa = 1$, $\eta = 1.276$, $\omega = 1$, $\omega' = 1$, $E = 0.03$, and dimensionless time $\tilde{t} = 1200$. The chain length is $N = 701$ site. Initially, the charge is within one site at the center of the chain. $u_n^0 = 0$ for all n.

field strength being the same. Let us take $|b_n(0)|$ in the form of the stretched inverse hyperbolic cosine:

$$|b_n(0)| = \frac{\sqrt{2}}{4}\sqrt{\frac{\kappa}{\xi|\eta|}}\cosh^{-1}\left(\frac{\kappa(n-n_0)}{4\xi|\eta|}\right), \qquad (11)$$

where ξ is the stretch factor.

Now we select the electric field strength so as to provide the uniform motion of the charge for $|b_n(0)|$ taken in the form of unstretched inverse hyperbolic cosine (6). Given E, we will gradually increase or decrease ξ. Up to some value of ξ ($\xi \neq 1$) depending on the parameter values, the initial stretched inverse hyperbolic cosine given by (11) quickly takes unstretched form (6) (or the form of the stationary charge distribution) in spite of the field counteraction. In this case, the charge, initially having executed a number of small oscillations, moves along the chain uniformly.

If the value of ξ is far from unity (for the given value of E), the charge loses its initial shape and, oscillating, moves in the chain in the direction of the field. In this case, the charge motion may be similar to the charge motion in the previous case; namely, if the charge distribution is taken in the form of unstretched inverse hyperbolic cosine (6), electric field strength E takes values at which the charge can not move uniformly. We used the phrase "may be similar," since the charge distribution may change markedly depending on the chain parameters.

CONCLUSIONS

We simulated the uniform charge motion for $\kappa = 1$ and $\eta = 1.276$. At these parameter values, the charge may move with a constant velocity in the chain in the direction of the field, retaining its shape. The uniform motion, as well as good agreement between the theoretical and numerically derived dependences of the charge velocity on the external field strength (Fig. 4), is due to the fact that the characteristic size of the polaron is $\lim_{\tilde{t}\to\infty} d(\tilde{t}) \approx 15$ for these parameters of the chain; that is, the polaron is wide and covers a large number of sites.

At large κ ($\kappa > 1$ for $\eta = 1.276$), the stationary polaron state of the charge "narrows." Because of this, for $\kappa = 2$ or greater than 2, Peierls–Nabarro oscillations associated with lattice imperfections [20] become noticeable. Thus, at $\kappa \geq 2$, the charge moves uniformly, weakly oscillating, and "periodically" retains its shape.

Computation shows that at $\kappa = 2$ and 3, as well as at $\kappa = 1$, the charge can move uniformly. More specifically, the charge uniform motion is possible only if

$E < E_{\text{max-numerical}}(\omega')$. For $E > E_{\text{max-numerical}}(\omega')$, the uniform motion of the charge is not observed; the initial shape of the charge distribution "decays"; and the charge, oscillating with a Bloch period, moves along the chain in the direction of the field. It is worth noting that the charge oscillation amplitude at the beginning of motion is close to the maximal amplitude of Bloch oscillations.

A uniform sequence of PolyG/PolyC nucleotide pairs is associated with coupling constant $\kappa = 4$ and matrix elements of site-to-site transfer $\eta = 1.276$ [23, 24]. These parameter values are assigned to the stationary polaron distribution of the charge [25] occupying only a few sites; that is, the polaron distribution has the form of a very narrow peak. Therefore, the uniform charge distribution in such a chain is difficult to simulate. For example, for $\omega = 1$ and $\omega' = 1$, only one value of E, $E = 0.09$, is found at which the charge moves in the chain with a constant velocity in the direction of the field, executing small oscillations and retaining its shape. In lower fields ($E < 0.09$), the charge ceases to move (becomes quiescent), whereas in higher fields ($E > 0.09$), the charge "decays" and, oscillating, moves in the direction of the field. As before, these oscillations are Bloch oscillations.

Earlier [26], we considered Bloch oscillations in the Holstein model as a function of parameter κ. The same results were obtained later in [27], where Bloch oscillations were studied in the Perrard–Bishop–Holstein model. In addition to the charge motions and distributions in the chain described here, the possibility of the charge nonequilibrium motion in the PolyG/PolyC chain of DNA was demonstrated [28].

Computation data indicate that complex dynamic regimes may be implemented in the given system that depend on the system's parameters; frequency; friction coefficient; chain length; and characteristic size of the steady-state polaron, which, in turn, depends on the dimensionless electron–lattice coupling constant in the system. With the system's parameter fixed, one can control the types of motion and charge distribution in the system by varying only the charge initial distribution and initial electric field strength.

ACKNOWLEDGMENTS

This work was supported by the Russian Foundation for Basic Research (grant no. 16-07-00305) and the Russian Science Foundation (grant no. 16-11-10163).

This work was fulfilled using the computational power of the Joint Supercomputer Center of the Russian Academy of Sciences

REFERENCES

1. A. S. Davydov, J. Theor. Biol. **38**, 559 (1973).
2. A. S. Davydov, J. Theor. Biol. **66**, 379 (1977).
3. A. S. Davydov, *Solitons in Molecular Systems* (Reidel, Dordrect, 1985).
4. A. C. Scott, Phys. Rep. **217**, 1 (1992).
5. V. D. Lakhno, Int. J. Quantum Chem. **108**, 1970 (2008).
6. *Nanobioelectronics – for Electronics, Biology, and Medicine*, Ed. by A. Offenhäusser and R. Rinaldi (Springer, 2009).
7. A. J. Storm, J. Van Noort, S. De Vries, and C. Dekker, Appl. Phys. Lett. **9**, 3881 (2001).
8. P. J. De Pablo et al., Phys. Rev. Lett. **85**, 4992 (2000).
9. H. W. Fink and C. Schönenberger, Nature **398**, 407 (1999).
10. Y. Okahata, T. Kobayashi, K. Tanaka, and M. Shimomura, J. Am. Chem. Soc. **120**, 6165 (1998).
11. D. Porath, A. Bezryadin, S. De Vries, and C. Dekker, Nature **403**, 635 (2000).
12. L. Cai, H. Tabata, and T. Kavai, Appl. Phys. Lett. **77**, 3105 (2000).
13. K.-H. Yoo et al., Phys. Rev. Lett. **87**, 198102 (2001).
14. A. Y. Kasumov et al., Science **291**, 280 (2001).
15. A. Chepeliaskii et al., New J. Phys. **13**, 063046 (2011).
16. V. D. Lakhno, in *Self-Organization of Molecular Systems – From Molecules and Clusters to Nanotubes and Proteins*, Ed. by N. Russo, V. Ya. Antonchenko, and E. Kryachko (Springer, 2009), p. 255.
17. V. D. Lakhno, J. Biol. Phys. **26**, 133 (2000).
18. T. Holstein, Ann. Phys. **8**, 343 (1959).
19. V. D. Lakhno, Int. J. Quantum Chem. **110**, 127 (2010).
20. V. D. Lakhno and A. N. Korshunova, Eur. Phys. J. B **79**, 147 (2011).
21. A. N. Korshunova and V. D. Lakhno, Mat. Biol. Bioinf. **11** (2), 141 (2016).
22. A. N. Korshunova and V. D. Lakhno, Mat. Biol. Bioinf. **12** (1), 204 (2017).
23. A. A. Voityuk, N. Rösch, M. Bixon, and J. Jortner, J. Phys. Chem. B **104**, 9740 (2000).
24. J. Jortner, M. Bixon, A. A. Voityuk, and N. Rösch, J. Phys. Chem. B **106**, 7599 (2002).
25. V. D. Lakhno and A. N. Korshunova, Math. Biol. Bioinf. **5** (1), 1 (2010).
26. V. D. Lakhno and A. N. Korshunova, Eur. Phys. J. B **55**, 85 (2007).
27. E. Diaz, R. P. A. Lima, and F. Dominguez-Adame, Phys. Rev. B **78**, 134303 (2008).
28. A. N. Korshunova and V. D. Lakhno, Phys. E **60**, 206 (2014).

Translated by V. Isaakyan